Heliyon 9 (2023) e21195

Contents lists available at ScienceDirect

Heliyon

journal homepage: www.cell.com/heliyon

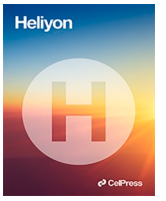

Potential of ultraviolet laser pulse-induced current for characterizing the grain size of table sugar

Xuecong Liu [a,c,d], Kun Zhao [b,c,d,*], Xinyang Miao [b,c,d], Honglei Zhan [b,c,d]

[a] College of Information Science and Engineering, China University of Petroleum, Beijing 102249, China
[b] College of New Energy and Materials, China University of Petroleum, Beijing 102249, China
[c] Beijing Key Laboratory of Optical Detection Technology for Oil and Gas, China University of Petroleum, Beijing 102249, China
[d] Key Laboratory of Oil and Gas Terahertz Spectroscopy and Photoelectric Detection, Petroleum and Chemical Industry Federation, China University of Petroleum, Beijing 102249, China

ARTICLE INFO

Keywords:
Laser-induced current
sugar
Grain
Laser-induced plasma
low power consumption

ABSTRACT

In this work, we proposed a laser-induced current (LIC) method to investigate the grain-size dependence of the plasma of table sugar induced by a nanosecond (ns) pulsed ultraviolet laser in the size range of <180 μm–>550 μm and achieve the lower power consumption in measurement. Under multiple laser irradiations and an external electric field (V_b) of 200 V, the LIC variation's (ΔI_p) standard deviation and variance were 0.53 nA and 0.05 nA, respectively, indicating the relatively small systematic error during the testing process. The V_b causes a decrease in the possibility of electron–ion complexation and accelerates the separation, resulting in an increase in ΔI_p with V_b. With increasing grain size (diameter D) of table sugar, ΔI demonstrate a valley-like behaviour and 250–380 μm is the critical range D_c where ΔI is very weak and considerably depends on the V_b with the slope of 0.031 nA/V. At $D > 550$ μm and $V_b = 5$ V, ΔI intensities monotonically rise by 30 % when D surpasses D_c. In this instance, the energy was the main contributor to the LIC signal during plasma generation and expansion. While D is less than D_c, ΔI_p increases by 27 % at $D \leq 180$ μm and $V_b = 5$ V. The yield stress is the main reason for the formation of plasma with high temperature and density in this situation because the sugar behaves like an elastic solid. The reason for such a LIC variation trend was discussed, which can be explained by considering the morphological, thermal and mechanical properties competing with each other. The present result suggests that the LIC method enables non-contact characterisation of sugar particle size at low-power consumption.

1. Introduction

Table sugar is found in almost every household throughout the world. White sugar, which is made from sugar beet or sugarcane and usually exists in the form of white crystals, is a type of sucrose with a high degree of purity. It contains two kinds of reducing monosaccharides, hexose and trace elements such as iron, copper and zinc [1]. It is not only a food and sweetener, but also an important pharmaceutical additive. Both fine white sugar (FS) and granulated sugar (GS) have the same composition according to the crystallisation states, but GS has a larger particle size. In contrast, brown sugar (BS) can only be extracted from sugarcane, and the composition of BS is more complex, consisting of a ketone, furanone, pyrazine, aldehyde, alcohol, acid, sulfur compounds and aromatic

* Corresponding author. College of New Energy and Materials, China University of Petroleum, Beijing 102249, China.
E-mail address: zhk@cup.edu.cn (K. Zhao).

https://doi.org/10.1016/j.heliyon.2023.e21195
Received 2 August 2023; Received in revised form 5 October 2023; Accepted 18 October 2023
Available online 19 October 2023

active compounds [2,3]. It can be used in cooking, baking and beverage industries. Different types of sugars have different application pathways.

Sugars play the most essential parts in food ingredients. China is not only one of the top 10 producers of sugar, but it is also a significant consumer market [4]. The grain size of table sugar is an important physical parameter reflecting the quality of sugar and directly affects the taste of table sugar and food. Taking GS as a sample, it is divided into coarse granulated sugar, medium granulated sugar, fine granulated sugar and young granulated sugar according to the granularity. The extensibility of the dough can be improved throughout the cookie-making process by increasing the size of the GS particles. When using only GS powder, the ductility is insufficiently high without being crisp, whereas when using only fine granulated sugar, the excessive ductility makes pattern-shaping difficult [5]. In addition, when sucrose is converted from a liquid phase to a solid phase with homogeneous particles, the sugar size can serve as a foundation for the optimisation of process parameters. Currently, most factories still use manual observation of sugar crystal growth to check the sugar production process [6]. This type of measurement has a significant amount of uncertainty and high individual variability. Due to a decline in their physical appearance, commercial sugar will experience pulverisation events during subsequent transportation [5]. The sugar size analysis is also crucial to scientifically elucidate the cause of the pulverisation of sugar crystals and improve their quality. As a result, the measurement of sugar particle size has important scientific significance and application value.

Laser-substance interaction is a complex process. The photoionisation phenomenon occurs when the laser energy exceeds the breakdown threshold of the sample itself and surface plasma is generated on the target surface. These plasmas contain ions, electrons and un-ionised neutral particles. After laser-induced plasma, optical, acoustical and electromagnetic phenomena are produced that reflect the features of the sample, allowing for the quantitative and qualitative analysis of the sample [7–14]. Although plasma can travel on material surfaces, it is difficult to observe the effect of surface plasma because of its short propagation distance. Since the separation of positive and negative charges under an external electric field to increase the plasma transmission distance on the surface is possible, it is possible to study the transport of plasma by detecting the surface voltage caused by charge separation, which was given the term laser-induced plasma transmission voltage (LIPTV) [15].

In addition to being a real-time method to be applied for characterising materials and monitoring reaction processes with high sensitivity and experimental simplicity, LIPT is sensitive to sample composition and structure [16–18]. Based on this feature, LIPT provided an application prospect in unconventional oil and gas resources, plasma dynamics detection and food inspection [19]. The spatial distribution and time evolution of the plasma can be reflected by LIPT signals in the meantime [20,21]. In recent years laser light technology has been explored in the field of food testing, such as biospeckle laser technique, Raman spectroscopies and laser-induced breakdown spectroscopy [22–25]. The characterisation of laser-induced plasma and the interactions between food and laser, however, are unclear.

To solve this question, we chose various types of sugar as samples for research [26]. According to the study, FS, GS and BS each have a unique LIPT response. FS showed higher LIPT than GS due to the smaller particle size of FS than that of GS, since the smaller size grain prefers to form a higher-temperature and higher-density plasma [27–30]. The sensitivity of LIPT to particle size offers ideas for solving the particle size detection problem of sugar in industrial production. The single-pulse deep ultraviolet laser detection characteristics of FS, BS and GS also allow them to match the remarkable requirements for an ultrafast response, high sensitivity and simple process. However, to ensure the high signal-to-noise ratio of LIPT response, a high applied bias of $V_b \geq 100$ V was used together with an oscilloscope whose precision for the voltage test was ~0.1 mV. One aim of the current study was to lower power consumption in measurement while taking into account the background. Since the Keithley 2400 m has a high sensitivity of ~0.1 nA, a LIC operating at a low bias was used to analyse the characteristics of sugar to fulfil the demand for low energy usage.

As is well known, the grain size of table sugar is a key parameter reflecting the quality, which has an important guiding value for the sugar industry. Although previous studies have shown that LIPT is sensitive to changes in particle size, it is unclear how response signal and grain size are related. The sugar industry is currently facing new challenges in environmental protection, automation control, low power, scientisation and global competition. Due to the limitation of oscilloscope accuracy, LIC was used in this work to characterise the grain size of sugar. Here, we carried out a specific experiment to measure the dependence of LIC of GS on the grain size over a range from <180 μm to >550 μm. The bias voltage was reduced to 5 V which is 1/20th of the lowest test bias of the LIPT [21].

2. Materials and methods

2.1. Materials

Commercial GS and BS were sourced from COFCO Croup in China as-supplied. Initially, the grain size of commercial sugar is randomly distributed. For the measurement of the dependence of LIC on the grain size, GS powders were fractionated by manual shaking for approximately 3 min using four sieves with mesh sizes of 550, 380, 250 and 180 μm, thus particle size classes were indicated with the corresponding grain diameter D of <180 μm, 180–250 μm, 250–380 μm, 380–550 μm and >550 μm. To confirm the accuracy of the experimental results, the samples were examined five times.

2.2. Measurements

Fig. 1 (a) shows the measurement system employed in this work. A KrF excimer laser from Coherent Inc. was used to irradiate the table sugar at room temperature in the air with an operating wavelength of 248 nm, a duration of 20 ns, a maximum pulse energy of 150 mJ, a maximum pulse frequency of 50 Hz, an average power of 7 W and a beam dimension of 14 × 7.5 mm^2. The LIC response is

derived from laser irradiation of sugar and the laser operates at 1 Hz. The fluctuation of single-plus laser energy is less than ±3 % over 10 pulses. The standard deviation is less than 0.002 %.

The sugar powder was evenly filled into a cuvette with a geometry of 20 mm × 45 mm and a thickness of 10 mm before the sample was exposed to radiation. The height of the sugar in the cuvette was 6.5 mm. Two parallel copper electrodes with 6 mm intervals were fixed in the cuvette. The laser irradiated onto the centre of the sample surface through a 10 mm × 7 mm diaphragm. The laser beam of area 70 mm^2 was half irradiated on table sugar and half irradiated in the air of the sample to ensure plasma evolution and propagation. The pulse energy E_{in} on the sample was 33.9 mJ. The electrodes were connected to the Keithley 2400 m. The Keithley 2400 m, which was also used to measure the current variation of table sugar under 248 nm laser irradiation, was used to generate a DC voltage V_b in the range of 0.5 V–200 V.

2.3. Equivalent circuit

The measurement system in Fig. 1(a) can be equated to a circuit in Fig. 1(b), where R_S and C_S are the time-varying plasma resistance and time-varying plasma capacitor of sugar, respectively. R_0 and C_0 are the line resistance and line capacitor, respectively. As shown in Fig. 1(c) a discharge channel is established by the initial plasma in the trigger process, and then the charged ions and electrons are separated under V_b, inducing the current increase from zero to a peak value after pulsed laser irradiation in the closing process [26]. The plasma features affect the discharge channel's impedance [31]. The sugar dimensional parameters can change the LIC by changing the value of R_S and C_S.

3. Results and discussion

Fig. 2 displayed the LIC signals of sugar at a bias V_b of 200 V with E_{in} = 33.9 mJ. The mean value, standard deviation and variance of LIC variation ΔI under 11 KrF excimer laser irradiation tests were 10.39 nA, 0.53 nA and 0.05 nA. The 95 % confidence interval for

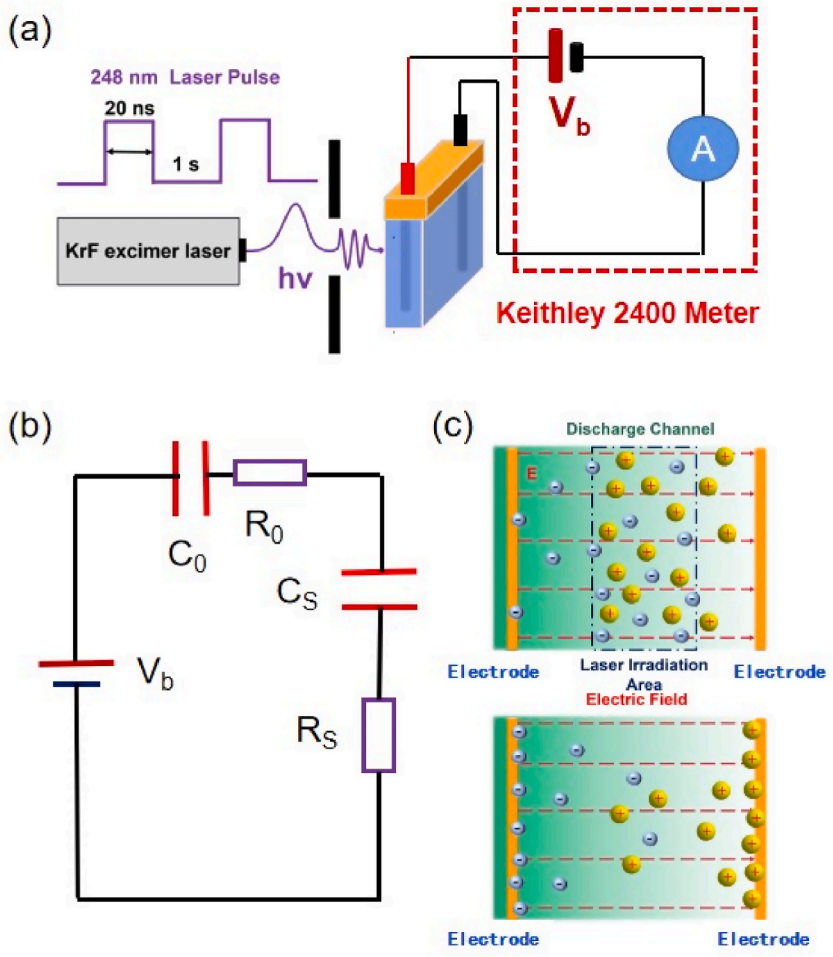

Fig. 1. Schematic diagram of (a) experimental arrangement, (b) equivalent testing circuit and (c) principle of LIC based on table sugar.

the mean is 10.25–10.55 nA, respectively. The selected trace was almost triangular and symmetrical with a peak value ΔI_P of ~10.25 nA. ΔI_P primarily reflected the quantitative characteristics of the laser-induced plasma. The 10%–90 % rising time t_r of ~0.09 s and a full-width at half-maximum of ~0.11 s are constrained by the testing software software's line response time and sampling rate. In this study, ΔI_P was used to characterise the LIC response of sugars with different grain sizes. The signal parameters are the mean of 11 single-pulse measurements to reduce the influence of laser energy variations and systematic errors on the LIC signals. The error bars were added to introduce standard deviation in the data point.

Fig. 3 shows the dependence of typical LIC variation ΔI_P on V_b when the KrF laser irradiated on the GS and BS with the on-sample energy $E_{in} \approx 33.9$ mJ. The ΔI_P increased monotonically from 0.04 to 10.5 nA and 0.025–7.8 nA with V_b from 0.5 to 200 V for GS and BS, respectively. The ΔI_P decreases linearly with V_b from 10 to 0.5 V at the slopes of ~0.081 and 0.07 nA/V for GS and BS, as can be observed in the inset of Fig. 3. As we know, white and brown sugar are significantly different in composition and structure. The non-centrifugation process imparts the products for BS, an incompletely purified cane sugar, with distinctive amino acids, phenolic acids and volatile phenols [32]. A high-energy pulse leads to the breaking of chemical bonds in sugar and finally the generation of plasma. GS and BS interact differently with laser because the strength of the hydrogen bonding network varies with the sugar structure. It has been found that the fragmentation of intramolecular sugar bonds preceded the breakdown of non-covalent complexes [33]. Due to the higher purity of sucrose in GS, a large number of sugar bonds are more likely to absorb the laser energy and break, resulting in a large amount of plasma. As a result, the LIC response for GS with higher sucrose purity than 99.9 % was greater than that of BS.

The sugar is ionised by intense laser pulses to produce electrons, charged ions atoms and molecules at electronically excited states [34]. As shown in Fig. 1(c), the plasma was initially concentrated at the laser irradiation position. Under the temperature and concentration gradients, electrons and charged ions are accelerated outward from the laser irradiation along the discharge channel. The lighter electrons are accelerated faster than the heavier ions [35]. The electrons will be the first to reach the vicinity of the electrode, forming a sheath and internal electric field that prevent electrons from approaching and encourage positive ions to neutralise some electrons. In this phase, the plasma is mainly affected by the temperature and concentration gradients primarily influence the expansion motion of the plasma. Charge separation results from the different rates at which electrons and ions expand in a plasma that has an internal electric field. Although, the density distributions of electrons and positive ions are the same, random collisions of electrons and positive ions will neutralise [19]. The excited electric dipole moment decreases with the recombination of electrons and ions. The applied electric field V_b accelerates the separation of electron and ion, reduces the recombination of electron and ion and leads to the increase of ΔI_P with the rise of V_b.

In the previous research [26], we discovered that various sugars may be categorised using the laser-induced voltage method. However, an external field greater than 100 V was applied to guarantee the sugar response signal's signal-to-noise ratio. Here, the LIC signal can satisfy the low-power requirements, in contrast to laser-induced voltage detection. The LIC variation ΔI_P as a function of V_b was displayed in Fig. 4 over the range from 0.5 to 100 V for the five-grain diameters. One can see a linear form of $\Delta I_P = aV_b$, where a = 0.048, 0.025, 0.031, 0.036 and 0.039 nA/V for $D \leq 180$ μm, $180 < D \leq 250$ μm, $250 < D \leq 380$ μm, $380 < D \leq 550$ μm and $D > 550$ μm, respectively. The LIC is weak for samples with grain sizes of $250 < D \leq 380$ μm, while out of this size value, an enhancement of the LIC is observed.

The charged particles in plasma exist randomly and expand outward from the laser irradiation region in the absence of an external electric field. Plasma clouds gathered on the sample indication absorb a portion of the laser energy as a result of the plasma shielding effect, resulting in a lower plasma number [36]. In addition to significantly reducing the plasma shielding effect, V_b also enhances plasma motion and distribution and increases the number of electrons reaching the electrodes [37]. As a result, as V_b increases, the amplitude of the LIC signal reaches a higher value. Here, the LIC can be measured at a smaller V_b than the laser-induced voltage test.

We plot the LIC variation ΔI_P versus the grain diameter D for the selected V_b in Fig. 5 to more clearly illustrate the LIC's dependence on grain size. It is observed that there is a valley-like behaviour in the ΔI_P with grain size D for each line V_b, and 250–380 μm is confirmed as a critical range D_c. When $D = D_c$, ΔI_P is very weak and significantly depends on the V_b. When D exceeds D_c, ΔI_P for $D >$ 550 μm abruptly increase by 73 % and 30 % stronger than that for $D = D_c$ at $V_b = 100$ and 5 V. While D is less than D_c, ΔI_P for $D \leq 180$ μm increase by 130 % and 27 % at $V_b = 100$ and 5 V.

Such a valley-like phenomenon suggests that the physical properties of the GS samples have changed about the grain size, leading to

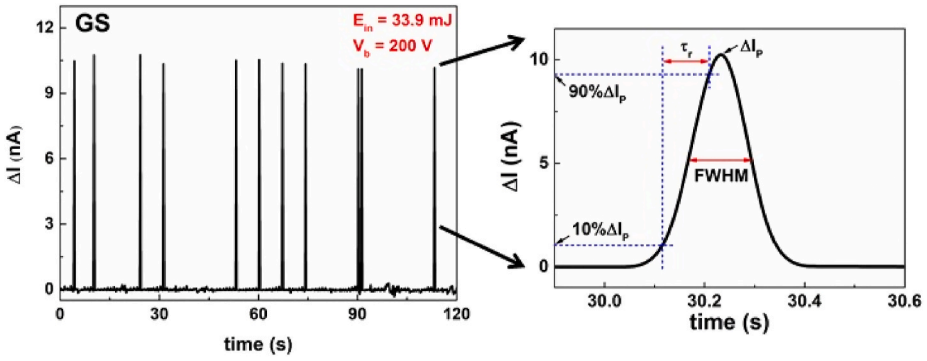

Fig. 2. LIC results ΔI of GS at $V_b = 200$ V under the irradiation of KrF laser with the on-sample energy $E_{in} \approx 33.9$ mJ.

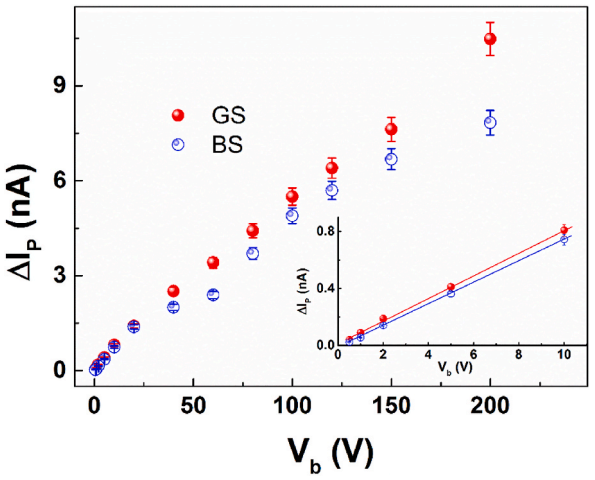

Fig. 3. Dependence of ΔI_P of GS and BS on V_b under the irradiation of KrF laser with the on-sample energy $E_{in} \approx 33.9$ mJ.

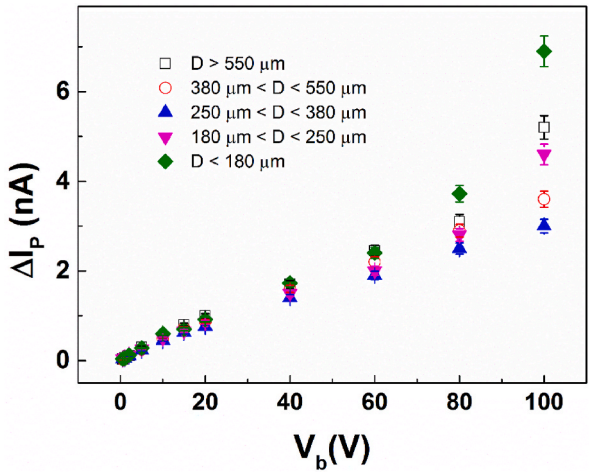

Fig. 4. Dependence of ΔI_P of GS grain on V_b under the irradiation of KrF laser with the on-sample energy $E_{in} \approx 33.9$ mJ.

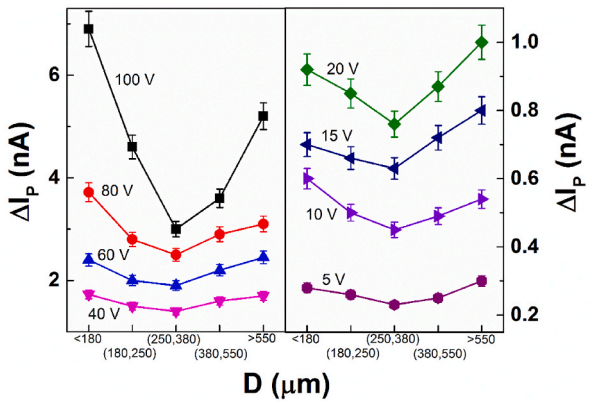

Fig. 5. Dependence of ΔI_P of GS grain on grain diameter D under selected V_b.

quite different situations of plasma formation. Differences in scattering efficiency among the samples are insignificant because the involved grain sizes are significantly larger than the laser wavelength. Previous research demonstrated that the plasma emissions depend on the crystal size and the smaller size grain leads to a higher vaporisation efficiency in laser ablation and the formation of a luminous plasma with higher temperature and higher density (Nakajima, 1984; [28–30]. Hence, when $D < D_c$, ΔI_P increases with D decrease. Additionally, it is well known that FS displayed higher LIPT than GS due to the smaller particle size of FS than that of GS [21]. These arguments suggest that the phenomenon below D_c the phenomenon below Dc may be explained by physical characteristics like morphology, such as surface roughness, and thermology, such as heat conductivity.

However, ΔI_P increases with increasing the particle size of sugar when D exceeds D_C, which is the opposite of the $D < D_c$ trend. It is reasonable to think of GS micrograin as a random randomly packed granular material to address this issue. As a type of typical soft matter that typically absorbs a certain portion of energy and particles that belong to the plasma during its generation, randomly packed granular material is frequently used in natural and industrial processes, such as dirt, sand and metal–non-metal powder. Since the randomly randomly packed granular material is a complex non-linear mechanical system varying dramatically between solid-like and fluid-like, it is inferred that the mechanical property plays a vital part in comprehending such a phenomenon above D_c. Smaller sizes usually lead to poorer mechanical performances [28]. As a result, the specific grain-size D_c represents a threshold, above which the yield stress of the GS grain is greater than the impact pressure exerted by the energy process of plasma generation and expansion. As a result, when $D > D_c$, it behaves like an elastic solid to help the formation of plasma with high temperature and density, resulting in higher LIC. Regardless of the mechanism, the LIC signal is primarily influenced by the number of plasmas. The trend of the measured ΔI_P with sugar particle size was unaffected by the change in bias voltage. The effect of V_b on ΔI_P was consistent with the previous discussion, where it only improves the signal-to-noise ratio of LIC. As a result, precise trends that indicate grain-size characterisation are provided by the LIC signal at lower applied biases.

Recently, using sieved copper microspheres with discrete diameters, ranging from 49 to 390 μm, as examples, it was discovered that the dependency of plasma emission on grain size exhibits a step-like phenomenon [28]. Such a phenomenon can be explained by considering the randomly randomly packed granular material as a non-Newtonian fluid with yield stress and effective viscosity. In contrast, the morphological, thermal and mechanical properties compete with each other and ultimately a valley-like phenomenon is produced in our current study. Further work is still needed for a better understanding of the role of each parameter in such a valley-like phenomenon.

Table sugar is an essential ingredient in people's diets. In the sugar industry, the table sugar's grain size is a crucial factor that affects the end product's product. White and BS are sensitive to KrF pulsed laser since it is known that table sugar has an absorption band in the ultraviolet range of around 250 nm [38]. In this study, KrF laser irradiation table sugar is used to characterise the properties of sugar by detecting LIC signal parameters. In recent years, techniques such as biospeckle laser, vis-NIR spectroscopy, chemometric approach, infrared spectroscopy, X-ray imaging, hyperspectral imaging and thermal imaging have been applied to relevant detection in the food field with innovative results [22,23,39–41]). Laser pulse-induced current is a relatively new non-invasive, low-cost and simple technique. This work achieves the characterisation and evaluation of samples by detecting the plasma generated after laser irradiation of the samples, in contrast to the detection theory of the biospeckle laser approach. With improved signal-to-noise ratios for LIC signals in an external electric field, the LIC signal parameter shows a valley-like phenomenon with a grain size of sugar. Here, 250–380 μm is confirmed as a critical range D_c. Although the main goal of this work was to characterise sugar grain size, there is still the issue of the low precision and single characterisation parameter $\Delta I_{P,}$ which needs to be further investigated in the future.

4. Conclusions

The sugar size analysis is crucial to improve their quality. In this study, we innovatively explored the highly sensitive and simple LIC method in the characterisation of sugar particle size. Combining the influence of the grain size of sugar on the LIC response and the laser-sugar interaction mechanism was used to illustrate the mechanism from the laser-induced plasma and a test equivalent circuit model was established. V_b played a role in improving the signal-to-noise ratio of the LIC signal and achieved an increase in LIC variation by increasing the amount of plasma that reaches the test electrodes and decreasing the opportunity for electron–ion complexation. Morphological, thermal and mechanical factors all have an impact on the LIC fluctuation with table sugar grain size. When $D < 250–380$ μm, the LIC decreases with increasing particle size due to the thermal and kinetic characteristics of the plasma. We can approximate it as an elastic solid subject to yield stress for $D > 250–380$ μm, and the LIC increases as D increases. The model has the potential to be a basis for the automatic control system in the batch sugar crystallisation process to reduce human labour. The LIC method has the potential to be implemented in the sugar particle size characterisation process to reduce human labour.

Funding statement

This research was supported by the National Natural Science Foundation of China under Grant 12374412.

Data availability statement

Data will be made available on request.

CRediT authorship contribution statement

Xuecong Liu: Writing – original draft, Investigation. **Kun Zhao:** Supervision, Methodology, Conceptualization. **Xinyang Miao:** Writing – review & editing. **Honglei Zhan:** Investigation.

Declaration of competing interest

The authors declare that they have no known competing financial interests or personal relationships that could have appeared to influence the work reported in this paper.

References

[1] T. Vu, J. LeBlanc, C.C. Chou, Clarification of sugarcane juice by ultrafiltration membrane: toward the direct production of refined cane sugar, J. Food Eng. 264 (2020), 109682, https://doi.org/10.1016/j.jfoodeng.2019.07.029.

[2] M. Polovková, P. Šimko, Determination and occurrence of 5-hydroxymethyl-2-furaldehyde in white and brown sugar by high performance liquid chromatography, Food Control 78 (2017) 183–186, https://doi.org/10.1016/j.foodcont.2017.02.059.

[3] J. Liu, P. Wang, C. Xie, D.W. Chen, Key aroma-active compounds in brown sugar and their influence on sweetness, Food Chem. 345 (2021), 128826, https://doi.org/10.1016/j.foodchem.2020.128826.

[4] P. Singh, Y.G. Ban, L. Kashyap, A. Siraree, J. Singh, Sugar and Sugar Substitutes: Recent Developments and Future Prospects, 2020, pp. 39–75, https://doi.org/10.1007/978-981-15-6663-9_9.

[5] M. Otsuka, Y. Hayashi, K. Miyazaki, M. Mizu, M. Okuno, T. Sasaki, Quality evaluation of white sugar crystals using the friability test and their non-destructive prediction using near-infrared spectroscopy, J. Drug Deliv. Sci. Technol. 82 (2023), 104390, https://doi.org/10.1016/j.jddst.2023.104390.

[6] J.L. Zhang, Y.M. Meng, J.F. Wu, J. Qin, H. Wang, T. Yao, S.S. Yu, Monitoring sugar crystallization with deep neural networks, J. Food Eng. 280 (2020), 109965, https://doi.org/10.1016/j.jfoodeng.2020.109965.

[7] N. Giannakaris, P. Siozos, V. Piñon, S.P. Banerjee, M. Sentis, J.D. Pedarnig, D. Anglos, UV femtosecond single-pulse and collinear double-pulse laser-induced breakdown spectroscopy (LIBS) for depth-resolved characterization of nano-scaled films, Appl. Surf. Sci. 640 (2023), 158354, https://doi.org/10.1016/j.apsusc.2023.158354.

[8] S. Shin, X. Wu, V. Patsekin, I.J. Doh, E. Bae, J. Robinson, B. Rajwa, Analytical approaches for food authentication using LIBS fingerprinting, Spectrochim. Acta B Atom Spectrosc. 205 (2023), 106693, https://doi.org/10.1016/j.sab.2023.106693.

[9] V.C. Costa, D.V. de Babos, F.W.B. de Aquino, V. Alex, F.A.C. Amorim, E.R. PereiraFilho, Direct determination of Ca, K and Mg in cassava flour samples by laser-induced breakdown spectroscopy (LIBS), Food Anal. Methods 11 (7) (2018) 1886–1896, https://doi.org/10.1007/s12161-017-1086-9.

[10] V.C. Costa, J.P. Castro, D.F. Andrade, D.V. de Babos, J.A. Garcia, M.A. Sperança, E.R. Pereira-Filho, Laser-induced breakdown spectroscopy (LIBS) applications in the chemical analysis of waste electrical and electronic equipment (WEEE), Trends Anal. Chem. 108 (2018) 65–73, https://doi.org/10.1016/j.trac.2018.08.003.

[11] V.C. Costa, F.A.C. Amorim, D.V. Babos, E.R. Pereira-Filho, Direct determination of Ca, K, Mg, Na, P, S, Fe and Zn in bivalve mollusks by wavelength dispersive X-ray fluorescence (WDXRF) and laser-induced breakdown spectroscopy (LIBS), Food Chem. 273 (2019) 91–98, https://doi.org/10.1016/j.foodchem.2018.02.016.

[12] T. Maruthaiah, S.K. Vajravelu, V. Kaliyaperumal, D. Kalaivanan, Soil texture identification using LIBS data combined with machine learning algorithm, Optik 278 (2023), 170691, https://doi.org/10.1016/j.ijleo.2023.170691.

[13] R.G. Raimundo, C.C. Vinícius, A.S. Marco, R.P. Edenir, Laser-induced breakdown spectroscopy (LIBS) and wavelength dispersive Xray fluorescence (WDXRF) data fusion to predict the concentration of K, Mg and P in bean seed samples, Food Res. Int. 132 (2020), 109037, https://doi.org/10.1016/j.foodres.2020.109037.

[14] S.J. Wu, L. Xue, M.Y. Yao, M.Q. Huang, Y.Q. Zeng, B.H. Huang, M.H. Liu, J. Li, Effect of cavity-confinement and microwave-assistance on the sensitivity of LIBS for detecting Cu content in pig feed, Optik 281 (2023), 170800, https://doi.org/10.1016/j.ijleo.2023.170800.

[15] Z.H. Meng, J. Zhu, H.L. Zhan, S.Z. Zhang, M.X. Chen, R. Chen, K. Zhao, W.Z. Yue, Influence of component and structure on laser induced voltage in sandstone, AIP Adv. 9 (2019), 115206, https://doi.org/10.1063/1.5128200.

[16] S.Z. Zhang, J. Zhu, H.L. Zhan, Z.H. Meng, R. Chen, H.Q. Liang, K. Zhao, W.Z. Yue, Laser-induced voltage application for identification of crude oils, Energy Fuels 33 (2019) 3855–3858, https://doi.org/10.1021/acs.energyfuels.8b03959.

[17] S.Z. Zhang, X.Y. Miao, H.L. Zhan, K. Zhao, H.Q. Liang, W.Z. Yue, Characterization of low- water-content crude oils under laser irradiation, Laser Phys. Lett. 17 (2020), 106002, https://doi.org/10.1088/1612-202X/aba908.

[18] S.Z. Zhang, X.R. Sun, C.L. Liu, H.Y. Zhang, X.Y. Miao, K. Zhao, Characterization of wax appearance temperature of model oils using laser-induced voltage, Phys. Fluids 34 (2022), 067123, https://doi.org/10.1063/5.0098727.

[19] X.C. Liu, Z.H. Meng, K. Zhao, X.Y. Miao, H.L. Zhan, S.Z. Zhang, Electrically tunable laser-induced voltage of coffee, IEEE Trans. Instrum. Meas. 72 (2023), 7006309, https://doi.org/10.1109/TIM.2023.3300417.

[20] X.Y. Miao, Q.D. Qin, Z. Liu, S.Z. Zhang, H.L. Zhan, K. Zhao, Determining the spatial distribution of laser-induced plasma by laser-induced voltaic measurement, Laser Phys. Lett. 18 (2021), 096003, https://doi.org/10.1088/1612-202X/ac1e85.

[21] X.C. Liu, K. Zhao, X.Y. Miao, Z.H. Meng, Z.H. Meng, Ultrafast ultraviolet laser-induced voltage of air, Opt Laser. Technol. 166 (2023), 109678, https://doi.org/10.1016/j.optlastec.2023.109678.

[22] N.K. Mahanti, R. Pandiselvan, K. Kothakota, S.P. Ishwarya, S.K. Chakraborty, M. Kumar, D. Cozzolino, Emerging non-destructive imaging techniques for fruit damage detection: image processing and analysis, Trends Food Sci. Technol. 120 (2022) 418–438, https://doi.org/10.1016/j.tifs.2021.12.021.

[23] R. Pandiselvam, V.P. Mayookha, A. Kothakota, S.V. Ramesh, R. Thirumdas, P. Juvvi, Biospeckle laser technique – a novel non-destructive approach for food quality and safety detection, Trends Food Sci. Technol. 97 (2020) 1–13, https://doi.org/10.1016/j.tifs.2019.12.028.

[24] C. Qu, Z.Y. Li, S.S. Du, Y.C. Geng, M.K. Su, H.L. Liu, Raman spectroscopy for rapid fingerprint analysis of meat quality and security: principles, progress and prospects, Food Res. Int. 161 (2022), 111805, https://doi.org/10.1016/j.foodres.2022.111805.

[25] M. Markiewicz-Keszycka, X. Cama-Moncunill, M.P. Casado-Gavalda, Y. Dixit, R. Cama-Moncunill, P.J. Cullen, C. Sullivan, Laser-induced breakdown spectroscopy (LIBS) for food analysis: a review, Trends Food Sci. Technol. 65 (2017) 80–93, https://doi.org/10.1016/j.tifs.2017.05.005.

[26] X.C. Liu, K. Zhao, X.Y. Miao, H.L. Zhan, Tunable laser-induced voltage of sugar for ultrafast ultraviolet laser pulse detection, IEEE Sensor. J. 23 (12) (2023) 12752–12758, https://doi.org/10.1109/JSEN.2023.3270903.

[27] M.L. Jiang, H. Liu, S.Y. Qiu, S.L. Min, Y.L. Gu, W.J. Kuang, J. Hou, Irradiation damage and corrosion performance of proton irradiated 304 L stainless steel fabricated by laser-powder bed fusion, Mater. Char. 202 (2023), 113023, https://doi.org/10.1016/j.matchar.2023.113023.

[28] X.L. Li, Y.J. Li, S.T. Li, M.J. Zhou, L.W. Chen, J. Meng, D.B. Qian, J. Yang, S.F. Zhang, Y. Wu, X.W. Ma, Steplike behavior in grain-size-dependent optical emission of plasma induced by laser-ablating granular material, Phys. Rev. Appl. 16 (2021), 024017, https://doi.org/10.1103/PhysRevApplied.16.024017.

[29] S. Li, Y. Li, X. Li, L. Chen, D. Qian, S. Zhang, Estimation of grain size in randomly packed granular material using laser-induced breakdown spectroscopy, Chemosensors 10 (4) (2022) 144, https://doi.org/10.3390/chemosensors10040144.

[30] C.E. Von Seggern, R.J. Cotter, Fragmentation studies of noncovalent sugar–sugar complexes by infrared atmospheric pressure MALDI, J. Am. Soc. Mass Spectrom. 14 (10) (2003) 1158–1165, https://doi.org/10.1016/S1044-0305(03)00478-1.

[31] L. Qin, C. Liu, R.X. Zhang, Y.O. Zhang, X.D. Yang, W.S. Zhao, Characterization of plasma discharge channel in EDM using photography and spectroscopy, Procedia CIRP 113 (2022) 184–189, https://doi.org/10.1016/j.procir.2022.09.129.
[32] E.B. Chen, H.L. Song, S.N. Zhao, C. Liu, L. Tang, Y. Zhang, Comparison of odor compounds of brown sugar, muscovado sugar, and brown granulated sugar using GC-O-MS, LWT 142 (2021), 111002, https://doi.org/10.1016/j.lwt.2021.111002.
[33] C.E.V. Seggern, R.J. Cotter, Fragmentation studies of noncovalent sugar–sugar complexes by infrared atmospheric pressure MALDI, J. Am. Soc. Mass Spectrom. 14 (10) (2003) 1158–1165, https://doi.org/10.1016/S1044-0305(03)00478-1.
[34] A. Elhambakhsh, V.D.L. Nguyen, L. Pradeep, V. Hessel, Recent progress and future directions in plasma-assisted biomass conversion to hydrogen, Renew. Energy 218 (2023), 119307, https://doi.org/10.1016/j.renene.2023.119307.
[35] Y.M. Huang, S. Xu, L.J. Yang, S.B. Zhao, Y. Liu, Y.S. Shi, Defect detection during laser welding using electrical signals and high-speed photography, J. Mater. Process. Technol. 271 (2019) 394–403, https://doi.org/10.1016/j.jmatprotec.2019.04.022.
[36] J.C. Li, W. Zhang, H.Y. Zheng, J.G.C. Jiang, Reducing plasma shielding effect for improved nanosecond laser drilling of copper with applied direct current, Opt Laser. Technol. 163 (2023), 109372, https://doi.org/10.1016/j.optlastec.2023.109372.
[37] H.X. Wang, J. Liu, Y. Xu, X.L. Wang, N.F. Ren, X.D. Ren, Q.X. Hu, Experimental characterization and real-time monitoring for laser percussion drilling in titanium alloy using transverse electric field assistance and/or lateral air blowing, J. Manuf. Process. 62 (2021) 845–858, https://doi.org/10.1016/j.jmapro.2020.12.051.
[38] N.D. Yordanov, V. Gancheva, E. Georgieva, EPR and UV spectroscopic study of table sugar as a high-dose dosimeter, Radiat. Phys. Chem. 65 (3) (2002) 269–276, https://doi.org/10.1016/S0969-806X(02)00210-4.
[39] R. Pandiselvam, R. Kaavya, S.I.M. Monteagudo, V. Divya, S. Jain, A.C. Khanashyam, A. Kothakota, V.A. Prasath, S.V. Ramesh, N.U. Sruthi, M. Kumar, M. R. Manikantan, C.A. Kumar, A.M. Khaneghah, D. Cozzolino, Contemporary developments and emerging trends in the application of spectroscopy techniques: a particular reference to coconut (cocos nucifera L.), Molecules 27 (10) (2022) 3250, https://doi.org/10.3390/molecules27103250.
[40] R. Kaavya, R. Pandiselvam, M. Mohammed, R. Dakshayani, A. Kothakota, A. V, D. Ramesh Cozzolino, C. Ashokkumar, Application of infrared spectroscopy techniques for the assessment of quality and safety in spices: a review, Appl. Spectrosc. Rev. 55 (7) (2020) 593–611, https://doi.org/10.1080/05704928.2020.1713801.
[41] R. Pandiselvam, N.K. Mahanti, M.R. Manikantan, A. Kothakota, S.K. Chakraborty, S.V. Ramesh, P.P.S. Beegum, Rapid detection of adulteration in desiccated coconut powder: vis-NIR spectroscopy and chemometric approach, Food Control 133 (2022), 108588, https://doi.org/10.1016/j.foodcont.2021.108588.